[1]Madhu Sudan Das
[2*]Usha Rani Gogoi
[3]Sanjoy Mandal

Efficient Adaptive Graph Velocity based Sliding mode Controller for path tracking of wheeled mobile robot in unknown environment

Journal of Electrical Systems

***Abstract* —** In this paper adaptive sliding mode controller (ASMC) is designed based on the kinematics of the wheeled mobile robots, while the second controller graph velocity based sliding mode controller (GVSMC) is designed based on dynamic behavior of wheeled mobile robots (WMR). Finally, adaptive neuro-fuzzy inference system (ANFIS) obstacle avoidance algorithm is used to generate a control signal and integrated with control signal of the GVSMC. These combined control action derives WMR for efficient path tracking and obstacle avoidance. Both controller ASMC and GVSMC guarantees stability of the system. Lyapunov stability is used in derivation of both control algorithms to ensure the stability. Proposed ASMC-GVSMC controller shows efficient performance for various path tracking over conventional sliding mode control and, Iterative learning control, and PID controller. Performance of the controllers are measured by the performance index IAE, ISE, STD of tracking error. Performance index simulation results using MATLAB / Simulink show that proposed control algorithm improves the performance of WMR for path tracking significantly. Proposed ASMC-GVSMC controller outperforms to the other existing sliding mode controller, iterative control and PID in navigation in obstacle environment.

Keywords: Sliding mode controller, Iterative learning, adaptive sliding mode controller, wheeled mobile robot (WMR), adaptive neuro-fuzzy inference system (ANFIS)

I. INTRODUCTION

The system of robot manipulators is strongly coupled, time-variant, and nonlinear. Hochpräzise manipulations have attracted both academic and industrial interest in recent years. When it comes to manipulator joint tracking, researchers have made a number of breakthroughs. Several control algorithms have been proposed, including: sliding mode, adaptive, resilient, and iterative learning control. Control methods like feedback linearization, model predictive control, etc. were proposed in the paper. Prior control approaches, on the other hand, were only possible when the dynamics models were well-understood and understood. Unfortunately, obtaining the exact dynamic model in practice is extremely difficult or even impossible. Deshalb replacing a complex robot system's dynamics model with a rough one can be beneficial for several reasons. Firstly, complex dynamics models can be computationally intensive and may not be suitable for real-time applications or on resource-constrained hardware. A time-variant complex robot system may also have unknown disturbances. The working process on this study takes for several years [5-6].

For an exoskeleton robot, the Sliding mode controller (SMC) law can be applied using a fractional order operator or a fuzzy neural system because it is robust against external disturbances and unmolded dynamics. Aside from that, it has a high-performance trajectory tracking system. When it comes to SMC design, which selects a suitable sliding mode surface [7]. A number of advantages of SMC include its robustness to parameter variations and its insensitivity to disturbances, to name a few, are two examples. The SMC's job is to steer and maintain the system's trajectory on a sliding surface that has been predetermined in state space. Both adaptive and sliding mode control can be used in practice. Flexible structures' vibrations have been controlled by some adaptive sliding mode controllers based on smart materials [8].

As a result of its robustness, ease of implementation, and design implications, SMC has become a popular tool for dealing with uncertainty and disturbances. Uncertainty and disturbances can only be solved by using an extremely powerful switch, friction between mechanical components and high temperatures in the power circuit [9]. To be sure, there are many shortcomings with the classic SMC. A nonlinear sliding function instead of a linear sliding

[1] Associate Professor, Department of Computer Science Engineering, The Neotia University, Kolkata, West Bengal, India

[2]* Corresponding author: Assistant Professor, Department of Computer Science Engineering, The Neotia University, Kolkata, West Bengal

[3] Professor, Electrical Engineering Department, IIT Dhanbad, Jharkhand, India

function has been suggested and adopted to treat these obstacles [10]. Some of these methods of control are referred to as terminal sliding mode control (TSMC).

It has been suggested that a saturation function applies to sliding mode controller gains to eliminate chattering in the sliding mode control. Though simple, this method does not ensure output convergence. To estimate and compensate for external disturbances and uncertainty by using an observer is another common method for solving the sliding mode control chattering problem. But it only works well with constant or slow-changing disturbances. Using fuzzy logic control is another way to deal with sliding mode control's chattering issues. Fuzzy control is well-known for being fault-tolerant and for being able to approximate any continuous function that exists inside a small set. Control theory has a strong foundation for this feature, which is also known as the universal approximation property [11, 12]. Fuzzy control is particularly useful in scenarios where system dynamics are unpredictable or challenging to correctly model. This is because one of its main benefits is its independence from precise system models. Fuzzy control can successfully handle unforeseen disturbances or errors and adapt to a wide range of real-world applications thanks to its flexibility.

A robust controller is used to obtain accurate results by compensating for nonlinear dynamics and external disturbances in manipulator tracking [12]. Robust controller performs well in hazardous, or repetitive [14]. Therefore, robotic manipulator development has emerged as one of the most exciting areas in modern industry. Robot manipulator faces problem due its applications are confined to slow motion operations with no external interaction. In part, this is due to the low performance of the available controllers. Advanced control strategies are needed to improve the operational speed and improve the accuracy of operations. When it comes to controlling robotic manipulators, stability and robustness are key requirements since a controller is the most important part of the complex system. The system's complexity and uncertainty pose the greatest challenges in its motion and control. Therefore, modelling and analysis of robotic manipulators, as well as the implementation of control methods, are essential for achieving precision, good accuracy, and increased productivity [15]. Contribution to the papers are as follows:

- The main contribution is to design adaptive sliding mode controller with guaranteed stability for Nonholonomic Mobile Robot.
- Adaptive controller is designed based on the kinematics of the non-holonomic wheeled mobile robot. ASMC concerned with the mobile robot's kinematic
- Output of the controller is angular velocity and linear velocity which are derived with guaranteed system’s stability. Lyapunov stability criteria is used for stability checking of the system.
- ANFIS obstacle avoidance algorithm are used for tracking when robot navigate in the obstacle environment.

This paper is organised as the following way. Section II presents systematic literature review. Section III presents our proposed methodology. Simulation results and discussion are presented in section IV. The conclusion is presented in section V.

II. RELATED WORK

Samir Zeghlache et al. [16] proposed a coaxial octo-rotor helicopter control scheme considering the actuator faults. Each subsystem of the octo-rotor helicopter's rotor system has a fault-tolerant (FTC) controller based on FLC and SMC. Fuzzy controller has been proposed for avoiding difficult modelling, reduce effect of chattering in SMC, reduce number of rules, as well as ensure system reliability.

Zewei Zheng et al. [17] presented for robotic airships with unknown wind disturbances and parametric uncertainties. Sliding-mode adaptive control is used in robotic airships to ensure asymptotically convergence errors of trajectory tracking and estimations. Adaptive gain schemes for the controller gains are the key for avoiding off-line tuning. Unknown wind disturbances and uncertain physical parameters and can be removed by utilizing variable structure control (VSC).

R. Sakthivel et al. [18] proposes a fuzzy Takagi-Sugeno time-varying delay system with unknown uncertainties and perturbations. The Controller has been designed that takes into account uncertainty and disturbance estimates for the systems. When combined with Wirtinger integral inequalities, it is possible to derive a sufficient condition for reliable trajectory tracking. When linear matrix inequalities are solved, a more robust controller can be obtained.

Yunkai Zhu et al. [19] delivered the DOBFSMC strategy for an inverter with a single-phase PV grid connection. It is necessary to use a SMC for regulating the output voltage of DC-AC converter. Also, fuzzy systems that approximate the upper bounds on observation errors between observation value and actual disturbance can provide better performance of the control system.

In [20], to decompose the nonlinear spacecraft attitude dynamics system, T-S fuzzy modeling is applied. Fuzzy T-S fuzzy modelling technique stabilizes a spacecraft's attitude tracking control. There is a real-time external disturbance with an unknown bound, and this design uses the adaptive estimate technique to counteract it in real time. The integral sliding surface is asymptotically stable because of the defined matrix inequality. Because of this, a finite amount of time is required to reach the specific sliding surface.

.

III. PROPOSED METHODOLOGY

In this paper, adaptive sliding mode controller (ASMC) and graph velocity-based sliding mode controller (GVSMC) are developed for handling parametric uncertainty. Adaptive sliding mode controller (ASMC) is designed based on the kinematics of the wheeled mobile robots, while the second controller GVSMC is concerned with dynamic behavior of WMR. For the kinematic controller, ASMC has been developed to address the model's nonlinearities. Also, robust graph velocity based sliding mode controller (GVSMC) is designed to handle the dynamic behavior. At the end, an ANFIS obstacle avoidance algorithm is included to avoid collisions and improve the system's overall robustness. Both controllers ASMC and GVSMC guarantee stability of the system and improve system performance. Figure 1 illustrates the overview of the proposed method.

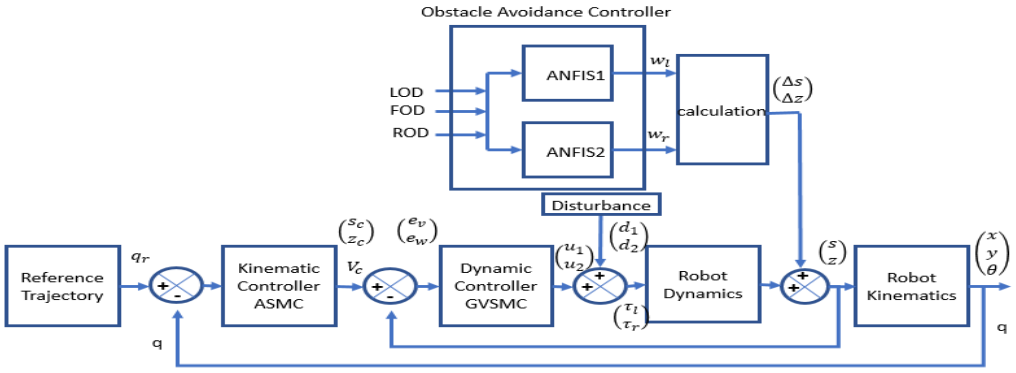

Fig.1 The proposed method

A. Kinematic Model

The mobile robot has two identical wheels mounted with a bar that can be controlled independently, shown in Figure 2. Here R represents wheel's radius and (x, y) is world cartesian coordinates of midpoint A. Midpoint A is on the axis between the center of the axis of left and right wheels and 2L represents axle length between the drive wheel. Mobile robot orientation is heading angle (rad). C is the robot's center of mass, which is on the axis of symmetry d distance from center A. Mobile robot's linear and the angular velocities are given by equation (1), and the kinematics of the mobile robot is given by the equation (2).

$$V = \frac{(VR+VL)}{2} = R\,\frac{(\dot{\emptyset}_R+\dot{\emptyset}_L)}{2} \tag{1}$$

$$W = \frac{(VR-VL)}{2L} = R\,\frac{(\dot{\emptyset}_R-\dot{\emptyset}_L)}{2}$$

$$\dot{q} = \begin{bmatrix}\dot{x}\\ \dot{y}\\ \dot{\theta}\end{bmatrix} = \begin{bmatrix}\cos\theta & 0\\ \sin\theta & 0\\ 0 & 1\end{bmatrix}\begin{bmatrix}v\\ w\end{bmatrix} \tag{2}$$

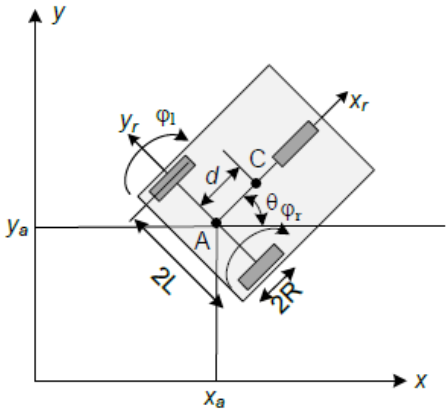

Fig. 2 Structure of WMR

B. Dynamic Mmodel of WMR

Dynamics of non-holonomic mobile robot is given as follows (Fukao et al., 2000):

$$M(q)\ddot{q} + V(q,\dot{q})\,\dot{q} + F(\dot{q}) + G(q) + \tau_d = B(q)\tau - \Lambda^T(q)^\gamma \tag{3}$$

$Q \in R^n$ represents generalized coordinates, $\tau \in R^n$ represents input vector, $\gamma \in R^n$ represents a vector of constraint forces, $V(q,\dot{q}) \in R^{nxn}$ centripetal and Coriolis matrix, $M(q) \in R^{nxn}$ indicates asymmetric and positive-definite inertia-matrix, $F(\dot{q}) \in R^n$ surface-friction matrix, $B(q) \in R^{rxn}$ represents input transformation matrix, and G(q) is gravitational vector, $\tau_d \in R^r$ indicates vector of unknown bounded disturbances, $\wedge(q) \in R^{mxn}$ represents a matrix associated the constraints. The equation (3) can be described as follows :

$$M(q)\ddot{q} + V(q,\dot{q})\,\dot{q} = B(q)\tau - \Lambda^T(q)^\lambda \tag{4}$$

Where $M(q) = \begin{bmatrix} m & 0 & -md\sin\theta & 0 & 0 \\ 0 & m & md\cos\theta & 0 & 0 \\ -md\sin\theta & md\cos\theta & I & 0 & 0 \\ 0 & 0 & 0 & 0 & 0 \\ 0 & 0 & 0 & 0 & I_w \end{bmatrix}$

$V(q,\dot{q}) = \begin{bmatrix} 0 & -md\dot{\theta}\cos\theta & 0 & 0 & 0 \\ 0 & -md\dot{\theta}\sin\theta & 0 & 0 & 0 \\ 0 & 0 & 0 & 0 & 0 \\ 0 & 0 & 0 & 0 & 0 \\ 0 & 0 & 0 & 0 & 0 \end{bmatrix}$, $B(q) = = \begin{bmatrix} 0 & 0 \\ 0 & 0 \\ 0 & 0 \\ 1 & 0 \\ 0 & 1 \end{bmatrix}$

$$\Lambda^T(q) = \begin{bmatrix} -\sin\theta & \cos\theta & \cos\theta \\ \cos\theta & \sin\theta & \sin\theta \\ 0 & L & -L \\ 0 & R & 0 \\ 0 & 0 & R \end{bmatrix} \text{x} \begin{bmatrix} \lambda_1 \\ \lambda_2 \\ \lambda_3 \\ \lambda_4 \\ \lambda_5 \end{bmatrix}$$

Now equation (4) can be expressed in another suitable for control and simulation. $\Lambda^T(q)^\lambda$ term is removed because λ_i (Lagrange multiplier) is unknown. It is possible by introducing reduce vector:

$$\dot{\eta} = \begin{bmatrix} \dot{\phi}_R \\ \dot{\phi}_L \end{bmatrix} \tag{5}$$

The forward kinematic model of the WMR is represented by equation (6) as follows:

$$\begin{bmatrix} \lambda_1 \\ \lambda_2 \\ \lambda_3 \\ \lambda_4 \\ \lambda_5 \end{bmatrix} = \frac{1}{2} \begin{bmatrix} \mathrm{R}\cos\theta & \mathrm{R}\cos\theta \\ R\sin\theta & R\sin\theta \\ R/L & -R/L \\ 2 & 0 \\ 0 & 2 \end{bmatrix} \begin{bmatrix} \dot{\phi}_R \\ \dot{\phi}_L \end{bmatrix} \tag{6}$$

The above equation can be represented as follows:

$$\dot{q} = \mathrm{S(q)}\eta \tag{7}$$

It can be proven that S(q) is the null space of the constraint matrix ∧(q). Therefore, we get equation (8) as follows:

$$\mathrm{S^T(q)}\wedge^{\mathrm{T}}(\mathrm{q}) = 0 \tag{8}$$

Differentiating the above equation:

$$\ddot{q} = \mathrm{S(q)}\eta + \mathrm{S(q)}\,\ddot{\eta} \tag{9}$$

Now equation (4) becomes:

$$\mathrm{M(q)}[\dot{S}(\mathrm{q})\ \eta\ + \mathrm{S(q)}\,\dot{\eta}\ ] + \mathrm{V(q,}\dot{q}\mathrm{)}[\ \mathrm{S(q)}\,\eta] = \mathrm{B(q)}\tau - \Lambda(q)^T\,\lambda \tag{10}$$

Rearranging it we get following:

$$\mathrm{S^T(q)M(q)S(q)}\ \dot{\eta} + \mathrm{S^T(q)[M(q)}\,\dot{S}(\mathrm{q})\ + \mathrm{V(q,}\dot{q}\mathrm{)S(q)]}\,\eta = \mathrm{S^T(q)B(q)}\,\eta - \mathrm{S^T(q)}\,\Lambda(q)^T\,\lambda \tag{11}$$

Now matrix defined as follows:

$$\bar{M}(\mathrm{q}) = \mathrm{S^T(q)M(q)S(q)} \tag{12}$$

$$\bar{V} = \mathrm{S^T(q)M(q)}\,\dot{S}(\mathrm{q})\ + \mathrm{S^T(q)}\ \mathrm{V(q,}\dot{q}\mathrm{)S(q)} \tag{13}$$

$$\bar{B} = \mathrm{S^T(q)B(q)} \tag{14}$$

The equation of the dynamics in reduced form is

$$\bar{M}(\mathrm{q})\ \dot{\eta} + \bar{V}(\mathrm{q},\dot{q})\,\eta = \bar{B}(\mathrm{q})\ \eta \tag{15}$$

where $\bar{M}(\mathrm{q}) = \begin{bmatrix} I_W + \frac{R^2}{4L^2}(mL^2 + I) & \frac{R^2}{4L^2}(mL^2 - I) \\ I_W + \frac{R^2}{4L^2}(mL^2 + I) & I_W + \frac{R^2}{4L^2}(mL^2 + I) \end{bmatrix}$ and

$\bar{V}(\mathrm{q},\dot{q}) = \begin{bmatrix} 0 & \frac{R^2}{2L}(m_c d\dot{\theta}) \\ \frac{R^2}{2L}(m_c d\dot{\theta}) & 0 \end{bmatrix}$ and $\bar{B}(\mathrm{q}) = \begin{bmatrix} 1 & 0 \\ 0 & 1 \end{bmatrix}$.

The dynamics of the WMR is represented by angular velocities $\dot{\phi}_R$, $\dot{\phi}_L$ and driving torques τ_R, τ_L, robot angular velocity $\dot{\theta}$. The equation (15) is expressed in angular and linear velocity(ω,υ) of WMR. The alternative form is given as follows:

$$(m + \tfrac{2I_w}{R^2})\ \dot{\upsilon} - \mathrm{m_c\,d}\ \omega^2 = \frac{1}{R}\ (\tau_R + \tau_L) \tag{16}$$

$$(I + \tfrac{2L^2 I_w}{R^2})\ \dot{\omega} - \mathrm{m_c\,d}\ \omega\ \upsilon = \frac{L}{R}\ (\tau_R - \tau_L) \tag{17}$$

C. Adaptive Sliding Mode Controller Design with guaranteed stability

In this section control algorithms u_1 and u_2 of ASMC will be evaluated for path tracking of desired trajectory which is

$$\dot{q} = \begin{bmatrix} \dot{x} \\ \dot{y} \\ \dot{\theta} \end{bmatrix} = \begin{bmatrix} \cos\theta & 0 \\ \sin\theta & 0 \\ 1 & 1 \end{bmatrix} \begin{bmatrix} v \\ w \end{bmatrix} \tag{18}$$

Let $x = x_1$, $y = x_2$, $\theta = x_3$, $v = u_1$ and $w = u_2$ kinematics of the robots becomes the following form

$$\dot{q} = \begin{bmatrix} \dot{x_1} \\ \dot{x_2} \\ \dot{x_3} \end{bmatrix} = \begin{bmatrix} \cos x_3 & 0 \\ \sin x_3 & 0 \\ 0 & 1 \end{bmatrix} \begin{bmatrix} u_1 \\ u_2 \end{bmatrix} \tag{19}$$

Rearranging the above kinematics equation, we can write

$$g_1(x_3)\, \dot{x_1} = u_1 \quad \text{where} \quad g_1(x_3) = \emptyset_1 \sec x_3 \tag{20}$$

$$g_2(x_3)\, \dot{x_2} = u_1 \quad \text{where } g_2(x_3) = \emptyset_2 \operatorname{cosec} x_3 \tag{21}$$

$\dot{x_3} = u_2 + d$ where d is disturbance.

Desired trajectory is x_d ,y_d and error $e_x = x_1 - x_d$, $e_y = x_2 - y_d$. Here defining sliding surface as follows:

$$s_1 = c_1 e_x + \dot{e_x} \quad \text{and } s_2 = c_2 e_y + \dot{e_y} \quad \text{where } c_1 > 0 \text{ and } c_2 > 0 \tag{22}$$

Lyapunov function is defined as

$$V_x = V_1 + V_2 \tag{23}$$

$$V_x = \frac{1}{2} g_1(x_3)\, s_1^{\,2} + \frac{1}{2\gamma_1} (\emptyset_1 - \hat{\emptyset}_1)^2 + \frac{1}{2\gamma_2} (\emptyset_2 - \hat{\emptyset}_2)^2 + \frac{1}{2\gamma_3} (\emptyset_3 - \hat{\emptyset}_3)^2 \tag{24}$$

where $V_1 = \frac{1}{2} g_1(x_3)\, s_1^{\,2}$

and $V_2 = \frac{1}{2\gamma_1} (\emptyset_1 - \hat{\emptyset}_1)^2 + \frac{1}{2\gamma_2} (\emptyset_2 - \hat{\emptyset}_2)^2 + \frac{1}{2\gamma_3} (\emptyset_3 - \hat{\emptyset}_3)^2$, $\gamma_i > 0$ and $\hat{\emptyset}_i$ is the estimation of $\emptyset_i$.

$$\dot{V_x} = \dot{V_1} + \dot{V_2} \tag{25}$$

Where $\dot{V_2} = \frac{1}{2\gamma} ((\emptyset_1 - \hat{\emptyset}_1)\dot{\hat{\emptyset}}_1$ (26)

Now differentiating above equation

$$\dot{V_1} = \frac{1}{2} \dot{g_1}(x_3)\, s_1^{\,2} + \frac{1}{2} g_1(x_3)\, s_1\, \dot{s_1} \tag{27}$$

$$= \frac{1}{2} \emptyset_1 \sec x_3 \tan x_3\, s_1^{\,2}\, \dot{x_3} + \emptyset_1 \sec x_3\, s_1 (c_1 \dot{e_x} + \ddot{e_x})$$

$$= \frac{1}{2} \emptyset_1 \sec x_3 \tan x_3\, s_1^{\,2}\, \dot{x_3} + \emptyset_1 \sec x_3\, s_1 (c_1 (\dot{x_1} - \dot{x_d}) + \ddot{e_x})$$

$$= \frac{1}{2} \emptyset_1 \sec x_3 \tan x_3\, s_1^{\,2}\, \dot{x_3} + \emptyset_1 \sec x_3\, s_1 (c_1 (\dot{x_1} - \dot{x_d}) + \ddot{x_1} - \ddot{x_d})$$

$$= \emptyset_1 [\frac{1}{2} \sec x_3 \tan x_3\, s_1^{\,2}\, u_2 + s_1 c_1 \sec x_3\, \dot{x_1} - s_1 c_1 \sec x_3\, \dot{x_d} + s_1 \ddot{e_x} \sec x_3]$$

$$= \emptyset_1 [\frac{1}{2} \sec x_3 \tan x_3\, s_1^{\,2}\, u_2 + s_1 c_1\, u_1 + s_1 c_1 d - s_1 c_1 \sec x_3\, \dot{x_d} + s_1 \ddot{e_x} \sec x_3]$$

For Lyapunov stability $\dot{V} < 0$. Control law is given below which guarantees the stability

$$u_1 = -\frac{\hat{\emptyset}_1}{c_1}[\frac{1}{2}\sec x_3 \tan x_3\, s_1 u_2 + c_1 \sec x_3\, \dot{x_d} - \ddot{e_x} \sec x_3] - K_1 \mathrm{sgn}(s_1) \quad (28)$$

Where K_1 is constant and $K_1 > = \max|c_1 d|$.

Putting this control law in the above equation that becomes

$$\dot{V}_1 = -K_1|s_1| - |c_1 d| - (\emptyset_1 - \hat{\emptyset}_1)[\frac{1}{2}\sec x_3 \tan x_3\, s_1{}^2 u_2 - s_1 c_1 \sec x_3\, \dot{x_d} + s_1 \ddot{e_x} \sec x_3] \quad (29)$$

Substituting in Lyapunov function

$$\dot{V_x} = \dot{V}_1 + \dot{V}_2 \quad (30)$$

$$= -K_1|s_1| - |c_1 d| - (\emptyset_1 - \hat{\emptyset}_2)[(\frac{1}{2}\sec x_3 \tan x_3\, s_1{}^2 u_2 - s_1 c_1 \sec x_3\, \dot{x_d} + s_1 \ddot{e_x} \sec x_3) - \frac{1}{\gamma_1}\dot{\hat{\emptyset}}_1] \quad (31)$$

The adaptive law is defined as in Eqn (32)

$$\dot{\hat{\emptyset}}_1 = \gamma_1(\frac{1}{2}\sec x_3 \tan x_3\, s_1{}^2 u_2 - s_1 c_1 \sec x_3\, \dot{x_d} + s_1 \ddot{e_x} \sec x_3) \quad (32)$$

Then $\dot{V_x} = -K|s| - |d| < 0$ which guarantees the stability. (33)

Now derivation of control algorithm u2 presented in the following section.

Following section presents derivation of sliding surface.

$$s_2 = c_2 e_y + \dot{e_y} \quad \text{where } c_2 > 0 \quad (34)$$

Lyapunov function is defined as

$$V_y = V_2 + V_3 \quad (35)$$

Where

$$V_2 = \frac{1}{2} g_2(x_3)\, s_2{}^2 \text{ and } V_3 = +\frac{1}{2\gamma_1}(\emptyset_1 - \hat{\emptyset}_1)^2 + \frac{1}{2\gamma_2}(\emptyset_2 - \hat{\emptyset}_2)^2 + \frac{1}{2\gamma_3}(\emptyset_3 - \hat{\emptyset}_3)^2 \quad (36)$$

$$V_y = \frac{1}{2} g_2(x_3)\, s_2{}^2 + \frac{1}{2\gamma_1}(\emptyset_1 - \hat{\emptyset}_1)^2 + \frac{1}{2\gamma_2}(\emptyset_2 - \hat{\emptyset}_2)^2 + \frac{1}{2\gamma_3}(\emptyset_3 - \hat{\emptyset}_3)^2 \quad \gamma_i > 0 \text{ and } \hat{\emptyset}_i \text{ is the estimation of } \emptyset_i. \quad (37)$$

Now derivative of Lyapunov function is defined as

$$\dot{V}_y = \dot{V}_3 + \dot{V}_4 \quad (38)$$

Where $\dot{V}_4 = \frac{1}{2\gamma}((\emptyset_2 - \hat{\emptyset}_2)\dot{\hat{\emptyset}}_2$ and

$$\dot{V}_3 = \frac{1}{2}\dot{g}_2(x_3)\, s_2{}^2 + \frac{1}{2} g_2(x_3)\, s_2\, \dot{s_2}$$

$$= -\frac{1}{2}\emptyset_2 \mathrm{cosec}\, x_3 \cot x_3\, s_2{}^2 \dot{x_3} + \emptyset_2 \mathrm{cosec}\, x_3\, s_2(c_2 \dot{e_y} + \ddot{e_y})$$

$$= -\frac{1}{2}\emptyset_2 \mathrm{cosec}\, x_3 \cot x_3\, s_2{}^2 u_2 + \emptyset_2 \mathrm{cosec}\, x_3\, s_2(c_2(\dot{x_2} - \dot{y_d}) + \ddot{e_y})$$

$$= -\frac{1}{2}\emptyset_2 \sec x_3 \tan x_3\, s_1{}^2 + \emptyset_2 \mathrm{cosec}\, x_3\, s_2(c_2(\dot{x_2} - \dot{y_d}) + \ddot{x_2} - \ddot{y_d})$$

$$= \emptyset_2[-\frac{1}{2}\mathrm{cosec}\, x_3 \cot x_3\, s_2{}^2 u_2 + s_2 c_2 u_1 - s_2 c_2 \mathrm{cosec}\, x_3\, \dot{y_d} + s_2 \ddot{e_y} \mathrm{cosec}\, x_3]$$

$$= \emptyset_2 s_2[-\frac{1}{2}\mathrm{cosec}\, x_3 \cot x_3\, s_2\, u_2 + c_2\, u_1 + c_2 d - c_2 \mathrm{cosec}\, x_3\, \dot{y_d} + \ddot{e_y} \mathrm{cosec}\, x_3]$$

For Lyapunov stability $\dot{V} < 0$. Control law is given below which guarantees the stability

$$u_2 = \frac{2\hat{\emptyset}_2}{s_2 \operatorname{cosec} x_3 \cot x_3 c_2} [c_2\, u_1 - c_2 \operatorname{cosec} x_3\, \dot{y_d} + \ddot{e_y} \operatorname{cosec} x_3 + K_2 \operatorname{sgn}(s_2)] \quad (39)$$

Where K_2 is constant and $K_2 >= \max|c_2 \mathrm{d}|$.

Putting this control law in the above equation that becomes

$$\dot{V}_3 = -\mathrm{K}|s_2| - |c_2 \mathrm{d}| - \frac{2(\emptyset_2 - \hat{\emptyset}_2)}{s_2 \operatorname{cosec} x_3 \cot x_3 c_2} [c_2\, u_1 - c_2 \operatorname{cosec} x_3\, \dot{y_d} + \ddot{e_y} \operatorname{cosec} x_3] \quad (40)$$

Substituting in Lyapunov function

$$\dot{V_y} = \dot{V}_3 + \dot{V}_4 \quad (41)$$

$$\dot{V_y} = -\mathrm{K}|s_2| - |c_2 \mathrm{d}| + \frac{2(\emptyset_2 - \hat{\emptyset}_2)}{s_2 \operatorname{cosec} x_3 \cot x_3 c_2} [c_2\, u_1 - c_2 \operatorname{cosec} x_3\, \dot{y_d} + \ddot{e_y} \operatorname{cosec} x_3 - \frac{1}{\gamma_2} \dot{\hat{\emptyset}}_2] \quad (42)$$

The Derivation of the adaptive law is demonstrated in the following section.

$$\dot{\hat{\emptyset}}_2 = \gamma_2 (c_2\, u_1 - c_2 \operatorname{cosec} x_3\, \dot{y_d} + \ddot{e_y} \operatorname{cosec} x_3) \quad (43)$$

ASMC control law for angular velocity and linear velocity are derived which guarantees the stability. Angular velocity control and Linear velocity and action are given as follows:

$$\mathrm{u}_1 = -\frac{\hat{\emptyset}_1}{\mathrm{c}_1}[\frac{1}{2} \sec \mathrm{x}_3 \tan \mathrm{x}_3\, \mathrm{s}_1 \mathrm{u}_2 + \mathrm{c}_1 \sec \mathrm{x}_3\, \dot{\mathrm{x}}_\mathrm{d} - \ddot{\mathrm{e}}_\mathrm{x} \sec \mathrm{x}_3] - K_1 \operatorname{sgn}(s_1) \quad (44)$$

$$u_2 = \frac{2\hat{\emptyset}_2}{s_2 \operatorname{cosec} x_3 \cot x_3 c_2} [c_2\, u_1 - c_2 \operatorname{cosec} x_3\, \dot{y_d} + \ddot{e_y} \operatorname{cosec} x_3 + K_2 \operatorname{sgn}(s_2)] \quad (45)$$

D. Graph Velocity Based Sliding Mode Controller (SVSMC)

Mobile robotics uses a directed graph such as D=1 to solve the communication problem (M, N, bij). Graph's weighted adjacency matrix is G. Bij explains the flow of state. 0 serves as the leader because it is an exogenous signal. BOJ>0 when (Mo, Mj) =N, otherwise not. There is no border between the leader and follower, so bij = 0. However, there is one caveat. This means a controller needs to be designed for maintaining formation while tracking the leader. Robot can also reach a particular target by using neighbor information. For example, we can write degout = $\sum$ j N bi for M. Our assumptions throughout this chapter are based on a single leader robot as the point of reference and a directional connection between it and the follower robots .Velocity can be calculated using equation (46) below, where d is the position and t is the time.

$$GV = \frac{\Delta d}{\Delta t} \quad (46)$$

An SMC system has a well-designed controller, which ensures that when the controller is activated, the states will shift towards desired sliding plan. Based on the Lyapunov technique, it has been shown that the system is stable. The system reaches to sliding surface in sliding mode control. In this mode, the dynamics of the system are constrained to remain on the sliding surface, resulting in robustness to disturbances and uncertainties.

$$M(u) = \begin{bmatrix} m_v \\ m_w \end{bmatrix} = e_e(u) + S \int_0^t e_e(\gamma) c\gamma, \quad (47)$$

where, $\mathrm{m_v}$ and $\mathrm{m_w}$ are given, respectively, by equation 6.21 and 6.22, $e_e = (s_c - s_m) = [e_v\, e_w]^Q$. with

$$e_v = s_c - s \text{ and } e_w = z_c - z,$$

The Graph Velocity Based Sliding Mode Controller is mathematically represented by the following conditions based on the above equation (47).

$$M_v(u) = GV[e_v(u) + S_v \int_0^t e_v(\gamma) c\gamma], \quad (48)$$

$$M_w(u) = \frac{\Delta d}{\Delta t} e_w(u) + S_w \int_0^t e_w(\gamma) c\gamma, \tag{49}$$

The sliding surfaces' derivatives, on the other hand, $M_v(u)$ and $M_w(u)$ are given by the following expressions;

$$\begin{aligned} \dot{M}_v(u) &= e_v(u) + S_v e_v(u), \\ \dot{M}_w(u) &= e_w(u) + S_w e_w(u). \end{aligned} \tag{50}$$

The dynamic motion of the root can be changed into

$$\dot{D}_m = (\bar{A}(p))^{-1} \bar{B}(q)\tau \tag{51}$$

Equation (51) may be written as

$$\dot{D}_m = \tilde{\tilde{B}}\tau \tag{52}$$

where $\tilde{\tilde{B}} = (\bar{A})^{-1} \bar{B}$

$\dot{D}_m = \tilde{\tilde{B}}\tau$

Switching and equivalent control laws are both used in the controller. Some other dynamics may be required in order to improve system stability and sliding mode stability, as well as to achieve a suitable system response and behaviour. Some dynamic systems may also require a controller that monitors measured signals in real-time. For tracking to be both robust and correct in the absence of measurement errors, the convergence time needs to be short.

E. Lyapunov Function based stability Analysis

Use Lyapunov theory to ensure that the robot is stable. Let us consider Lyapunov candidate function as:

$$SA = \frac{1}{2}e_1^2 + \frac{1}{2}e_2^2 + \frac{1}{2}e_3^2 \tag{53}$$

The derivative of lyapunov function is presented below,

$$\dot{S}A = \dot{e}_1 e_1 + \dot{e}_2 e_2 + \dot{e}_3 e_3,$$

$$\begin{aligned} \dot{S}A = (\sigma_1(ze_2 - s + s_d) + \sigma_2(ze_2 - s) + \sigma_3(ze_2 - s))e_1 + (\sigma_1(-ze_1 + s_d e_3) + \sigma_2(-ze_1 + s_d) \\ + \sigma_3(-ze_1 - s_d))e_2 + (\sigma_1(z_d - z) + \sigma_2(z_d - z) + \sigma_3(z_d - z))e_3. \end{aligned}$$

$$\dot{S}A = ((-s + \sigma_1 s_d))e_1 + \left(\sigma_1 s_d e_2 + z_d + (\sigma_2 - \sigma_3)\frac{s_d e_2}{e_3} - z\right)e_3. \tag{54}$$

Using angular velocities and linear velocities , the following results will be obtained;

$$\begin{aligned} SA_c &= L_1 e_1 + \sigma_1 s_d, \\ z_c &= \sum_{j=1}^{3} \sigma_j z_j = z_d + L_3 e_3 + \sigma_1 s_d e_2 + (\sigma_2 - \sigma_3)\frac{s_d e_2}{e_3} \end{aligned} \tag{55}$$

Equation (29) becomes;

$$\dot{S}A = -L_1 e_1^2 - L_3 e_3^2 \le 0, \qquad if\ e_3 \ne 0. \tag{56}$$

If $e_3 = 0$ then $\sigma_1 = 1$ and $\sigma_2 = \sigma_3 = 0$. So, $s_c = L_1 e_1 + s_d$ and $Z_c = \sum_{j=1}^{3} \sigma_j z_j = z_d + L_3 e_3 + s_d e_2$. Also,

$$\dot{S}A = -L_1 e_1^2 - L_3 e_3^2 \le 0. \tag{57}$$

Hence first order derivative of the lyapunov function is negative so the stability of the system is guaranteed. Simply following condition is checked for ensuring reaching condition is satisfied. The candidate Lyapunov function is is chosen as

$$SA = \frac{1}{2} Z^{Q} Z \tag{58}$$

The derivation can be expressed as;

$$\begin{aligned}
&\dot{S}\, A = Z^{Q} Z, \\
&\dot{S}\, A = Z^{Q} \left[\dot{S}_c - \tilde{\tilde{B}} \tau + S e_e(u) \right], \\
&\dot{S}\, A = Z^{Q} \left[\dot{S}_c - \tilde{\tilde{B}} \left(\tau_{eq} + \tau_z \right) + S e_e(u) \right], \\
&\dot{S}\, A = Z^{Q} \dot{Z} = Z^{Q} \left[\dot{Z}_c - \tilde{\tilde{B}} \left(\tau_{eq} + S e_e(u) \right) \right].
\end{aligned} \tag{59}$$

Finally, the system's stability was demonstrated using a Lyapunov approach based on stability analysis.

F. Obstacle avoidance algorithm

Two ANFIS controllers are used for obstacle avoidance as shown in Figure 3. Two ANFIS controllers are used. Input of the ANFIS controllers are left obstacle distance (LOD), front obstacle distance (FOD) and right obstacle distance (ROD). These LOD , ROD, FOD are the sensory information.

Output of two ANFIS are left angular velocity and right angular velocity respectively. At first obstacle avoidance ANFIS controller are trained with training data (Al-Mayyahi et al., 2014). 21 datapoints of FOD, LOD and ROD as input and respective output left angular velocity and right velocity are used for training. During trainig 200 epochs are used and gaussians membership function are chosen. Obtained Training error for w_r is 0.0121rad/sec and 0.0.321 for w_l. If obstacles are found in the robot path then velocity and orientation are modified to avoid the obstacle and reaches to the target. If there are no obstacles, then obstacle avoidance algorithm controller's output is zero. Only tracking control action will work.

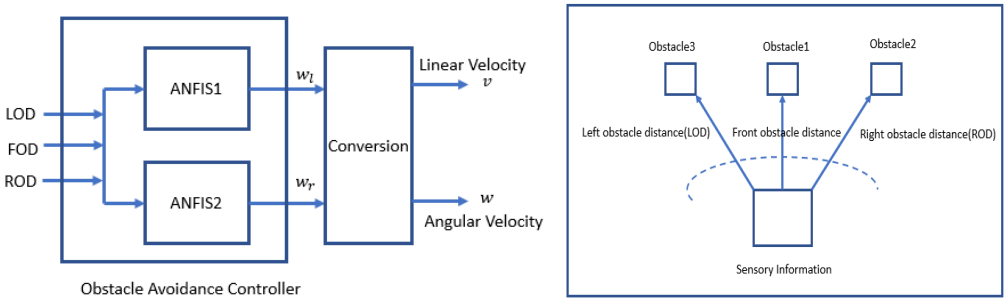

(a) (b)

Figure 3(a) Obstacle avoidance controller, (b) Sensory Information block

In the second stage AKH-NFIS is used as kinematic controller replacing KASMC and DASMC as dynamic controller. Architecture of intelligent controller AKH-NFIS are shown in Figure 4.

As depicted in Figure 4, NFIS refers to feed-forward-neural-network (FF-NN), KH optimization algorithm and NFIS is integrated together known as AKH-NFIS algorithm in the proposed work. To represent the NFIS architecture considers first-order Sugeno model which uses the following fuzzy rule:

Rule No.1: IF P is A_{11} AND Q is B_{11},

$$\text{Then, } F_{11} = u_{11} P + v_{11} Q + w_{11} \tag{60}$$

Rule No.2: IF P is A_{22} AND Q is B_{22}

$$\text{Then } F_{22} = u_{22}P + v_{22}Q + w_{22} \tag{61}$$

Where, A_{11} , A_{22} and B_{11}, B_{22} denotes membership functions for P← A_{jj} and Q← B_{jj} respectively. The parameter u_{11}, v_{11}, w_{11} and , u_{22}, v_{22}, w_{22} are learnable parameters of output functions. In the training phase, the value of these parameters are evaluated. The AKH-NFIS architecture comprises of five layers as illustrated in the Figure 4.

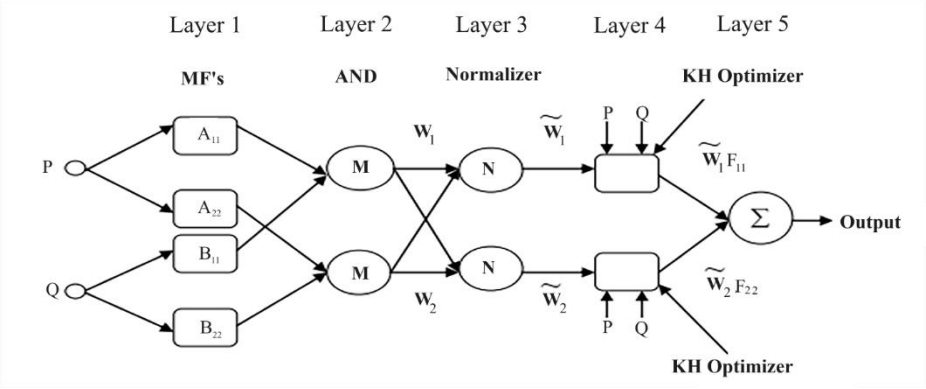

Figure 4: AKH-NFIS model

Layer 1: Each node's output of layer1 is presented by:

$$\boldsymbol{Ol_{1,i} = \mu_{Aii}(P)}\ i = 1,2 \tag{62}$$

$$\boldsymbol{Ol_{1,i} = \mu_{Bi-2}(Q)}\ i = 3,4 \tag{63}$$

Where, crisp input variable P, Q. These variables are fuzzified into linguistic variable and A_{ii} B_{ii}, represents membership values of the membership functions μA and μB respectively. Gaussian membership function are $\mu_{Aii}(P)$ and $\mu_{Bii}(Q)$ expressed as,

$$\mu(x) = e^{-\left(x-p_k/\sigma_k\right)^2} \tag{64}$$

Where, p_k and σ_k are mean and standard deviation of data.

Layer 2: Node is fixed in this layer which evaluates the firing strength of the rule given by equation (15). It is represented by M. The firing strength of this node is expressed by the following expression.

$$\boldsymbol{O_{2,j} = w_j = \mu_{Ajj}(P) * \mu_{Bjj}(Q)}\ \ j = 1,2 \tag{65}$$

Layer 3: Layer3 are also fixed nodes. It is indicated by N' . It normalizes preceding layer's firing strength . Output of the layer3 is expressed as:

$$O_{3,i} = \widetilde{w}_i = {}^{w_i}/_{(w_1 + w_2)} \quad \boldsymbol{i = 1,2} \tag{67}$$

Layer 4: Layer4 has adaptive nodes. The output of every nodes are normalized firing strength. Output of this node is first-order polynomial expressed as :

$$O_{4,j} = \widetilde{w}_j * F_j = \widetilde{w}_j(u_{jj}P + v_{jj}Q + w_{jj}) \quad \text{j=1,2} \tag{68}$$

Where, parameter u_{11}, v_{11}, w_{11} and u_{22}, v_{22}, w_{22} are consequent parameter. Here, krill herd optimization algorithm is used for updating these parameters.

Layer 5: Single node acts as basic adder and results are expressed as follows:

$$\boldsymbol{O_{5,i}} = \sum \widetilde{\boldsymbol{w}}_{\boldsymbol{i}} \boldsymbol{F_i} = (w_1 F_1 + w_1 F_1)/(w_1 + w_2\ ) = {\sum_{\boldsymbol{j}} \boldsymbol{w_i F_i}}\Big/{\sum_{\boldsymbol{i}} \boldsymbol{w_i}} \qquad (69)$$

Two AKHNFIS are used as kinematic controller. One output of AKH- NFIS is linear velocity (vc) and another output is angular velocity (wc).

IV. Results and Discussion

In this section simulation result of an ASMC for Nonholonomic Mobile Robot is presented. We consider three different trajectories in case1, case2 and case3. MATLAB software and computer with 6 GB RAM and an Intel I-7 processor are used for simulation purpose. At 2.6 GHz, the approach was tested for accuracy and efficiency of the performance.

In case 1 parameters are $c_1 = c_2$ = 10, $\gamma_1 = \gamma_2$ = 150, $\theta(0)$ = 0.01, $\omega(0)$ = 0, initial state of $\emptyset_1 = \emptyset_2 = 0$. Uncertainty d= 0.01sin(t) and various desired trajectory are considered.

Case1: Desired trajectory x and y position are given as

x_d = t + 0.1*sin(t), and yd = t + cos(t) respectively.

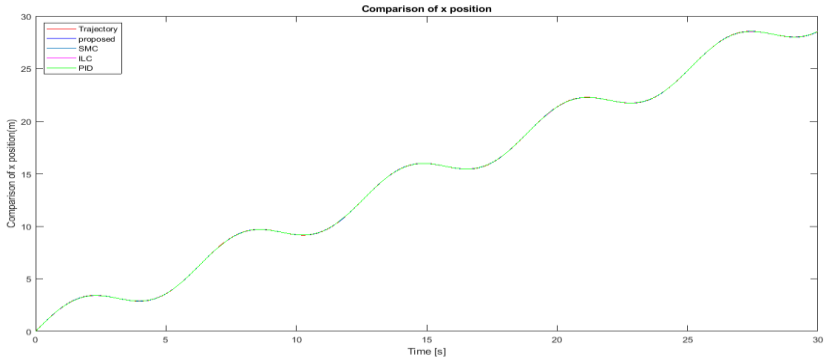

(a)

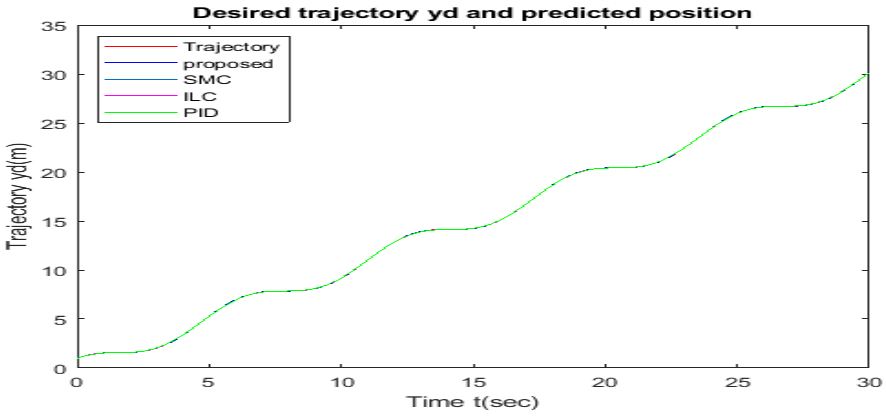

(b)

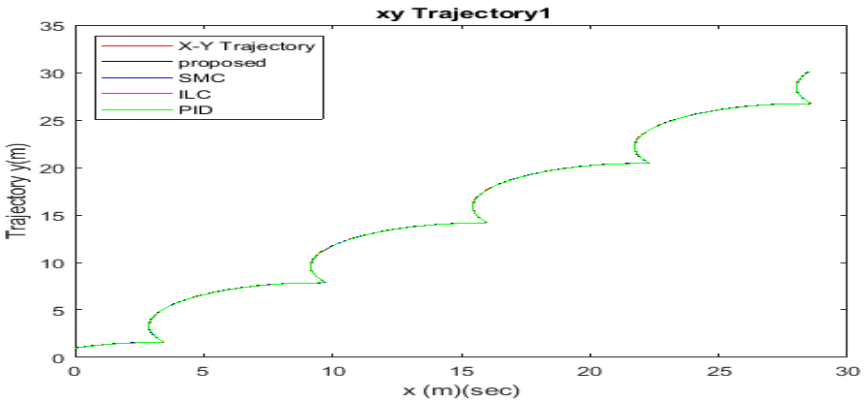

(c)

Figure 5. (a) Desired trajectory x_d , (b) Desired trajectory y_d , (c) Comparison of trajectory with proposed ASMC-GVSMC, SMC, ILC, and PID

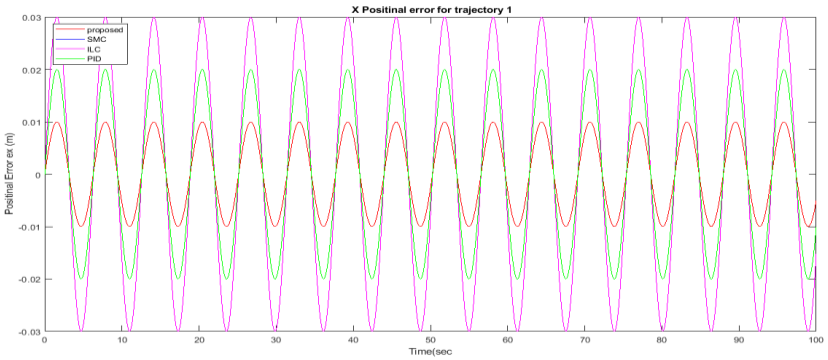

(a)

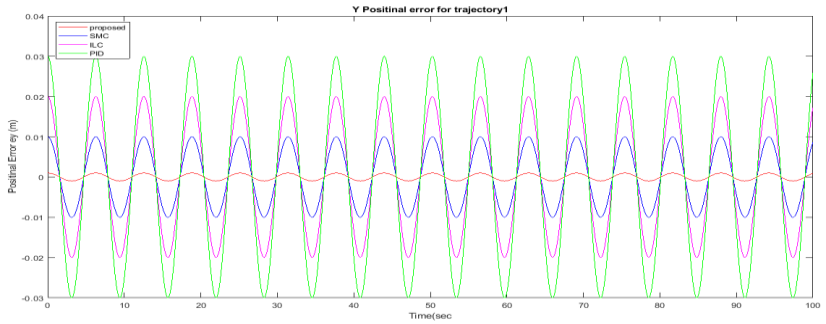

(b)

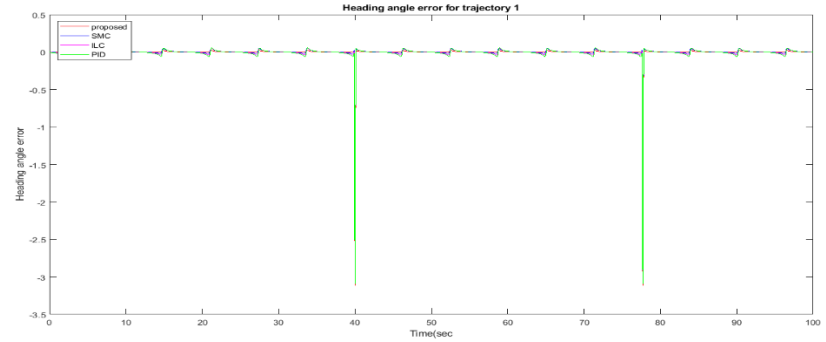

(c)

Figure 6. Comparison of position errors (a) e_x with ASMC-GVSMC, SMC, ILC, and PID, (b) e_y with ASMC-GVSMC, SMC, ILC, and PID and (c) Comparison of position errors heading angle error with ASMC-GVSMC, SMC, ILC, and PI

Fig. 6 (a), (b), (c), demonstrates tracking errors in case 1. Our proposed control method provides the highest tracking precision in case1. For positional error in x direction xe, as depicted in Fig. 6(a), errors are small level using the ASMC-GVSMC method, while the traditional PI, SMC, and ILC provides relatively high error. Furthermore, Fig. 6(b) shows positional error in x direction ye, errors is small level using the ASMC-GVSMC method, while the traditional PI, SMC, and ILC provides relatively high error respectively. In case1 the ASMC-GVSMC system guarantees smaller steady-state errors. Small trajectory error reaches the sliding surface with better convergence time and stay on it thereafter. Controlactions u1 and u2 and sliding surface s1 and s2 are shown in the following Figure 7.

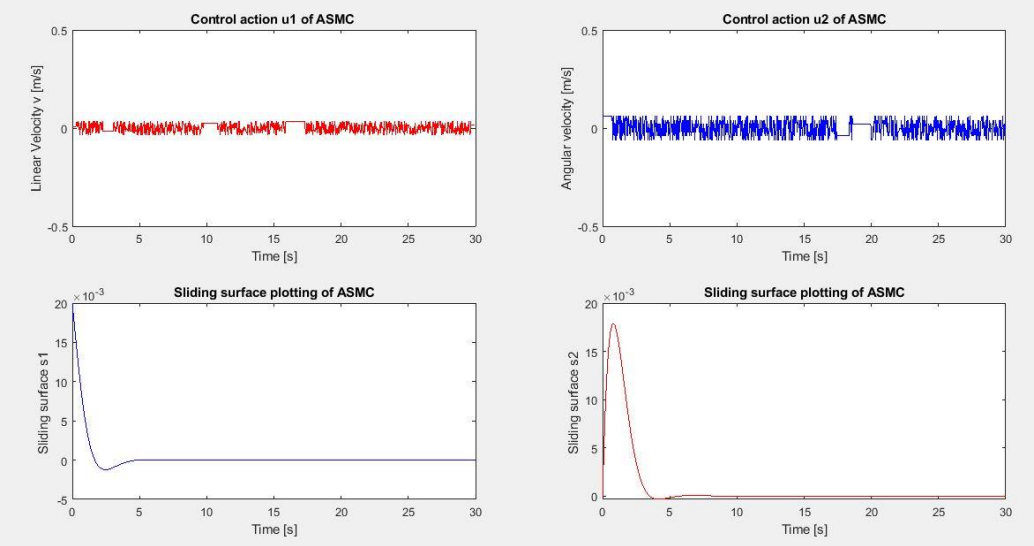

Figure 7. ASMC controller's output v and w and sliding surface s1 and s2 in case 1

Case 2: when desired trajectory is x = t + 10*sin(t) and y = t + 4*cos(t). In simulation $c_1 = c_2 = 15$, $\gamma_1 = \gamma_2 = 140$, $\theta(0) = 0.01$, $\omega(0) = 0$, initial state of $\emptyset_1 = \emptyset_2 = 0$, uncertainty d= 0.05sin(t) are considered. Figure 8, Figure 9, Figure 10 and Figure 11(a, b, c) shows various trajectories by proposed method, SMC, ILC, and PID.

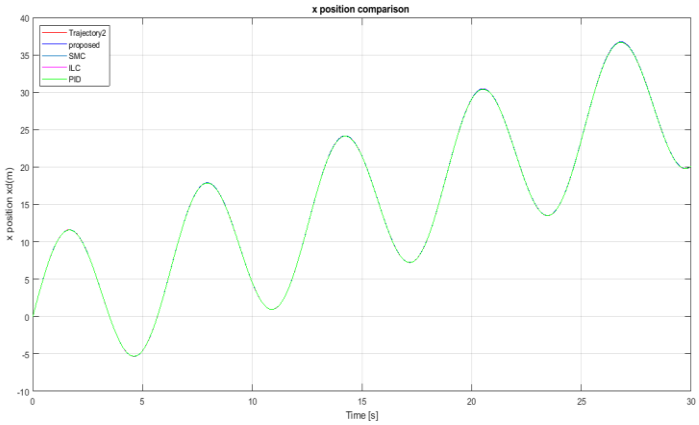

Figure 8. Desired trajectory x_d in case 2

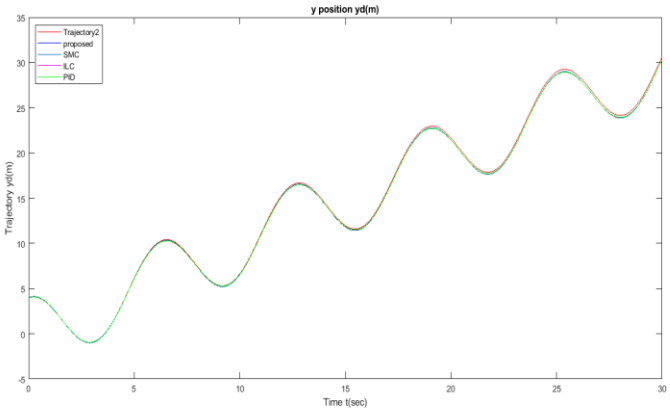

Figure 9. Desired trajectory y_d in Case 2

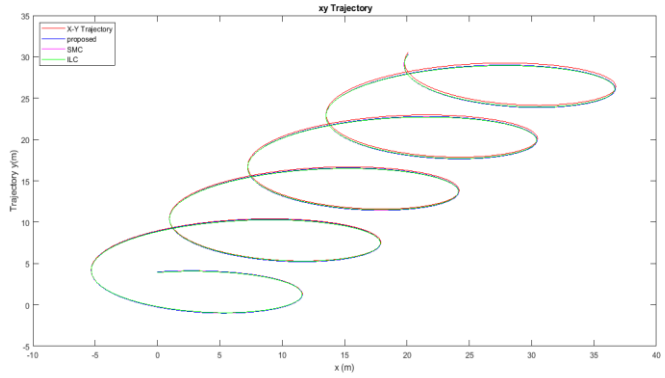

Figure 10. Comparison of trajectory with ASMC-GVSMC, SMC, ILC, PID

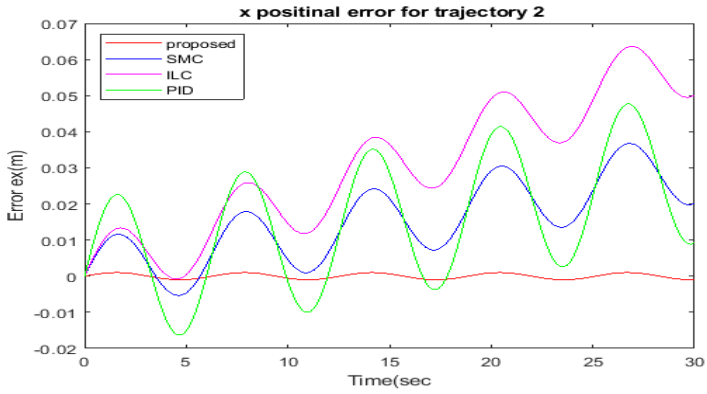

(a)

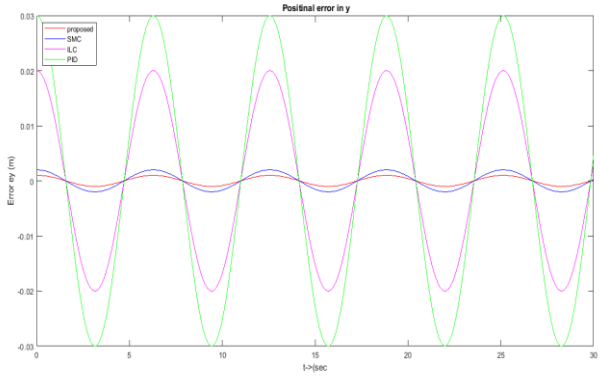

(b)

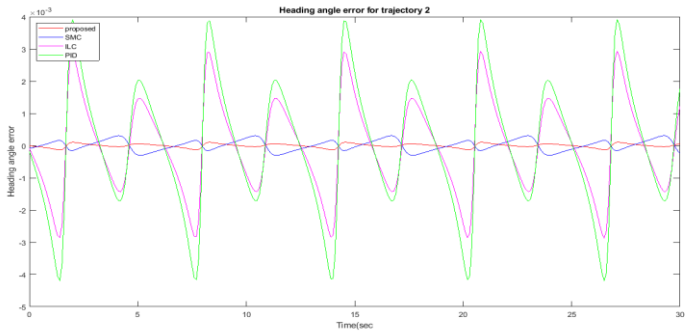

(c)

Figure 11. (a) Position error e_x comparison with SMC, ILC, PID, (b) Position error e_y comparison with SMC, ILC, PID and (c) Position error e_θ comparison with SMC, ILC, PID

The obstacle avoidance is done in that dynamic environment. The integral absolute error (IAE), integrated absolute error (ISE), and standard deviation (STD) of the absolute tracing errors are presented as quantitative criteria to effectively demonstrate the comparative performance.

Case 3: In case 3 parameters are $c_1 = c_2$ = 9, $\gamma_1 = \gamma_2$ = 130, $\theta(0)$ = 0.01, $\omega(0)$ = 0.01, initial state of $\emptyset_1 = \emptyset_2 = 0$. Uncertainty d= 0.06cos(t). Desired trajectory in case3 given as

x=t+10*sin(t) y = 0.5*t.*t+4*cos(t)

Figure 12 shows the desired trajectory of Case 3. Figure 13 shows the Control action v and w and sliding surface s1 and s2 of ASMC-GVSMC controller in Case 3.

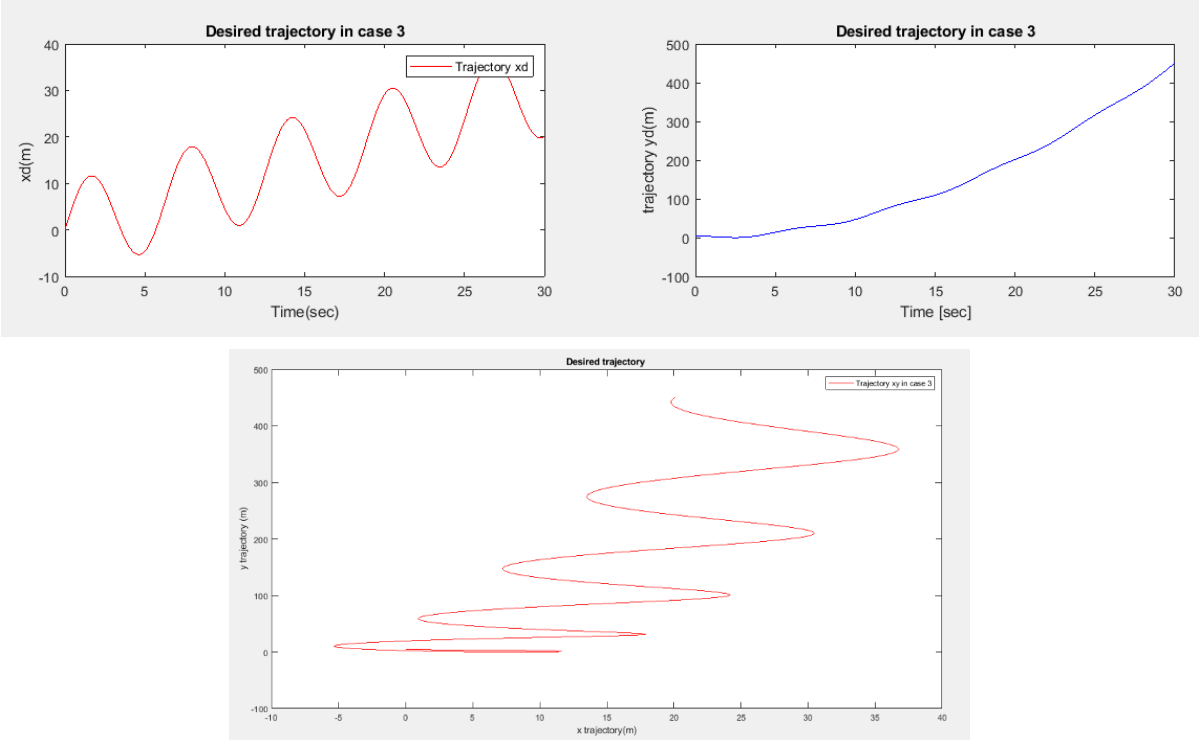

Figure 12. Desired Trajectory in case 3

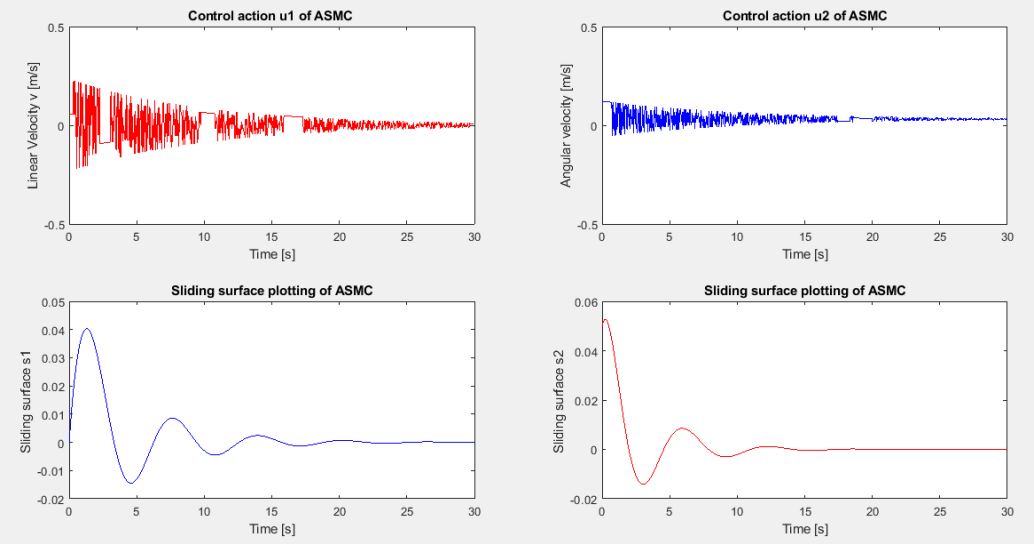

Figure 13. Control action v and w (above) and sliding surface s1 and s2 (below) ASMC-GVSMC controller in case3

Table 1: Tracking criteria of various control methods in case 1

Error	Measure	SMC	ILC	PID	Proposed
x_e	IAE	3.8408	5.7611	3.8408	1.9204
	ISE	0.0605	0.1361	0.0605	0.0151
	STD	0.0142	0.0213	0.0142	0.0071
y_e	IAE	1.9071	3.8141	5.7212	0.1907
	ISE	0.0150	0.0599	0.1348	0.00015
	STD	0.0070	0.0141	0.0211	0.0007
θ_e	IAE	2.9931	3.8973	4.9104	1.2565
	ISE	0.0648	0.0980	0.1573	0.0146
	STD	0.0140	0.0179	0.0229	0.0063

Table 1 shows that the proposed ASMC based methods could achieve more stable and precise tracking than standard SMC controllers, and that the created ASMC-GVSMC scheme has significantly enhanced capabilities. When using the proposed method to evaluate the ISE criterion, the related values with respect to ex, e_y, e_θ are withi 0.151m, 0.0001m, and 0.0146 rads, respectively. When using the proposed method to evaluate IAE related values with respect to ex, e_y, e_θ are within 01.9204m, 0.007m, 1.256rad. STD obtained for proposed method are 0.0071rad , 0.007rad, 0.0063rad .When compared to the traditional methods, proposed ASMC-GVSMC control strategy clearly achieves the least performance criteria in terms of statistics, indicating that the suggested ASMC is capable of managing tracking with decreased tracking errors and enhanced stability. Three tracking errors ex, e_y, e_θ have been reduced at least 50% using our proposed method.

Table 2: Tracking criteria of various control methods in case 2

Error	Measure	SMC	ILC	**PID**	Proposed
x_e	IAE	4.7463	9.1177	5.5772	0.1920
	ISE	0.1042	0.3741	0.1542	0.0002
	STD	0.0106	0.0181	0.0164	0.0007
y_e	IAE	11.4424	15.2566	19.0707	0.1907
	ISE	0.5391	0.9584	1.4975	0.0001
	STD	0.0423	0.0564	0.0705	0.0007
θ_e	IAE	0.0894	0.1808	0.3063	0.0123
	ISE	0.0351	0.2894	0.7066	0.0009
	STD	0.0003	0.0010	0.0015	0.0001

Table 2 shows that the proposed ASMC-GVSMC based methods could achieve more stable and precise tracking than standard SMC controllers, and that the created ASMC-GVSMC scheme has significantly enhanced capabilities. When using the proposed method to evaluate the ISE criterion, the related values with respect to ex, e_y , e_θ are within 0.0002m, 0.001m, and 0.009 rad, respectively. When using the proposed method to evaluate IAE related values with respect to ex, e_y , e_θ are within 0.1.90m, 0.1907m, 0.123 rad. STD obtained for proposed method are 0.0007m , 0.0001m, 0.0001 rad. When compared to the traditional methods, proposed ASMC-GVSMC control strategy clearly achieves the least performance criteria in terms of statistics, indicating that the suggested ASMC-GVSMC is capable of managing tracking with decreased tracking errors and enhanced stability. Three tracking errors ex, e_y , e_θ have been reduced at least 45% using our proposed method.

Table 3: Tracking criteria of various control methods in case 3

Error	Measure	SMC	ILC	PID	Proposed
x_e	IAE	3.6463	7.1167	4.6762	0.1130
	ISE	0.1143	0.2642	0.1452	0.0003
	STD	0.0216	0.0380	0.0362	0.0006
y_e	IAE	10.3624	13.1536	14.141	0.1732
	ISE	0.4281	0.8574	1.3874	0.0002
	STD	0.0323	0.0463	0.0614	0.0018
θ_e	IAE	0.0794	0.1746	0.2152	0.0112
	ISE	0.0242	0.2724	0.6163	0.0015
	STD	0.0004	0.0011	0.0014	0.0002

Table 3 shows that the proposed ASMC-GVSMC based methods could achieve more stable and precise tracking than standard SMC controllers, and that the created ASMC-GVSMC scheme has significantly enhanced capabilities. When using the proposed method to evaluate the ISE criterion, the related values with respect to ex, e_y , e_θ are within 0.0003m, 0.002m, and 0.0015rads, respectively. When using the proposed method to evaluate IAE related values with respect to ex, e_y , e_θ are within 0.1130m, 0.1732m, 0.0112 rad. STD obtained for proposed method are 0.0006m , 0.0018m, 0.0002. rad When compared to the traditional methods, proposed ASMC-GVSMC control strategy clearly achieves the least performance criteria in terms of statistics, indicating that the suggested ASMC-GVSMC is capable of managing tracking with decreased tracking errors and enhanced stability. Three tracking errors ex, e_y , e_θ have been reduced at least 50% using our proposed method.

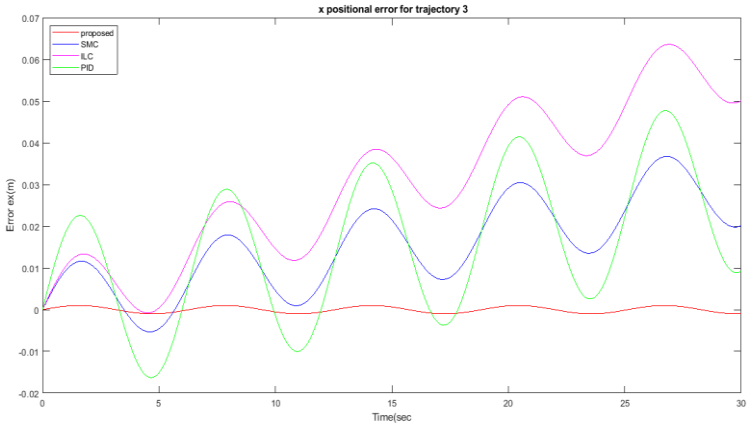

Figure 14. (a) Position error e_x comparison with SMC, ILC, PI

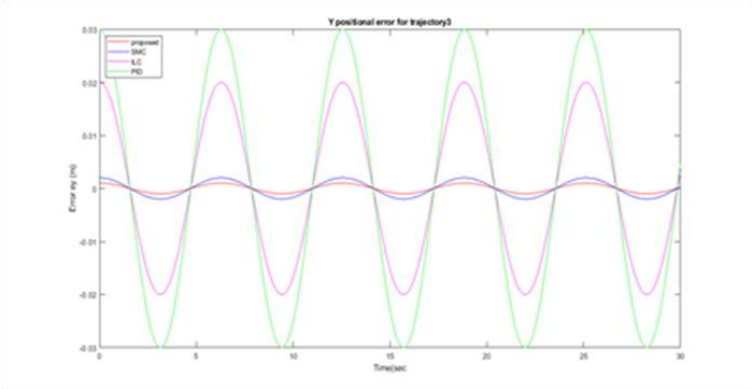

Figure 14. (b) Position error e_y comparison with SMC, ILC, PID

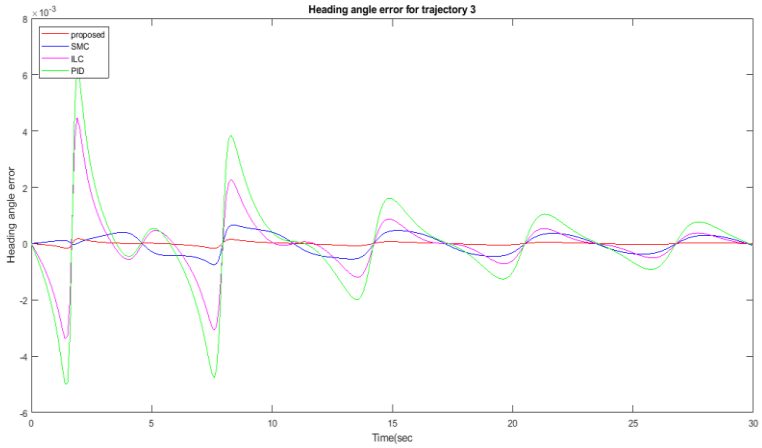

Figure 14(c) Position error e_θ comparison with SMC, ILC, PID

Case 4: Obstacle avoidance performance

ASMC-GVSMC works as a tracking controller where ANFIS controller is used as obstacle algorithm for navigation. Combined effect provides efficient path tracking in obstacle environment. Obstacle avoidance performance comparisons are given below in terms of length of trajectory (pathlength) and cost time. Results shows avoidance algorithm improves the performance of ASMC-GVSMC for path navigation in uncertainty. Figure 15 shows robot follows the desired path avoiding obstacle without collision effectively. Tracking path is much closer to the desired path for proposed method than others method. Pathlength and cost time are 11.69m and 27 sec respectively for proposed method which indicates average speed is 0.43m/. Overall cost time, path length and average speed is improved by the proposed method.

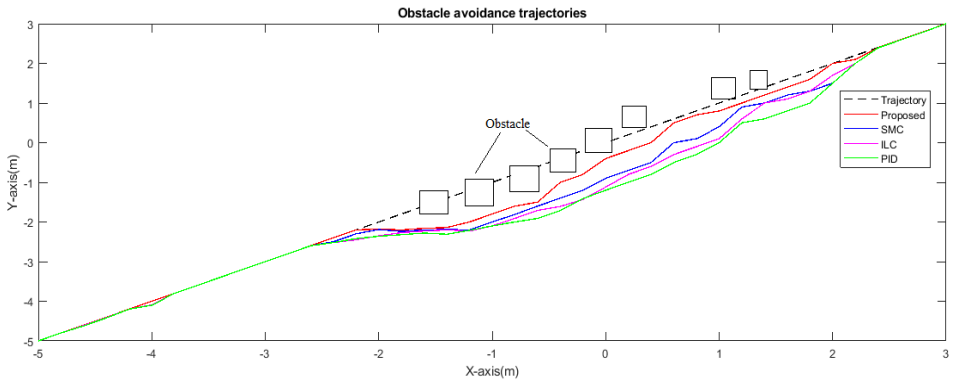

Figure 15. obstacle avoidance trajectories

Pathlength for various controllers proposed, SMC, ILC and PID are respectively 11.69m, ,11.72m, 11.76, and 11.80m respectively. From the Figure 15 it is observed that using the proposed control algorithm WMR can efficiently navigate in the obstacle environment. Lowest pathlength is required for the proposed method. It ensures that tracking controller ASMC-GVSMC efficiently track the path and avoid obstacle with the inclusion of obstacle avoidance algorithm (ANFIS).

V. CONCLUSION

This study, presents a control method of nonholonomic wheeled mobile robot for path tracking. Adaptive sliding mode controller (ASMC) is designed based on the kinematics of the wheeled mobile robots, while the second controller GVSMC is concerned with dynamic behaviour of WMR. ANFIS obstacle avoidance algorithm is included to avoid collisions and improve the system's overall robustness. Both controllers ASMC and GVSMC guarantees stability of the system and improves performance. From the simulation results of performance measuring index demonstrated above shows that proposed ASMC-GVSMC outperforms the existing approaches SMC, ILC, and PID.

ACKNOWLEDGMENT

The work presented herein was conducted at the School of Science and Technology of The Neotia University, Diamond Harbour Rd, Sarisha, West Bengal 743368, West Bengal.

REFERENCES

[1] S. Wang, L. Tao, Q. Chen, J. Na, and X. Ren, “USDE-based sliding mode control for servo mechanisms with unknown system dynamics,” IEEE/ASME Transactions on Mechatronics, vol. 25, no. 2, pp. 1056–1066, 2020.

[2] M. Tao, Q. Chen, X. He, and M. Sun, “Adaptive fixed-time fault-tolerant control for rigid spacecraft using a double power reaching law,” International Journal of Robust and Nonlinear Control, vol. 29, no. 12, pp. 4022–4040, 2019.

[3] V. T. Yen, W. Y. Nan, P. Van Cuong, N. X. Quynh, and V. H. .ich, “Robust adaptive sliding mode control for industrial robot manipulator using fuzzy wavelet neural networks,”International Journal of Control, Automation andSystems, vol. 15, no. 6, pp. 2930–2941, 2017.

[4] Q. Chen, H. Shi, and M. Sun, “Echo state network-based backstepping adaptive iterative learning control for strictfeedback systems: an error-tracking approach,” IEEE Transactionson Cybernetics, vol. 50, no. 7, pp. 3009–3022, 2020.

[5] Zheng, Kunming, Youmin Hu, and Bo Wu. "Intelligent fuzzy sliding mode control for complex robot system with disturbances." European Journal of Control 51 (2020): 95-109.

[6] K. Zheng , Y. Hu , B. Wu , X. Guo , New trajectory control method for robot with flexible bar-groups based on workspace lattices, Robot. Auton. Syst. 111 (2019) 44–61.

[7] Rahmani, Mehran, and Mohammad Habibur Rahman. "An upper-limb exoskeleton robot control using a novel fast fuzzy sliding mode control." Journal of Intelligent & Fuzzy Systems 36, no. 3 (2019): 2581-2592.

[8] Fang, Yunmei, JuntaoFei, and Tongyue Hu. "Adaptive backstepping fuzzy sliding mode vibration control of flexible structure." Journal of Low Frequency Noise, Vibration and Active Control 37, no. 4 (2018): 1079-1096.

[9] Truong, Thanh Nguyen, Anh Tuan Vo, and Hee-Jun Kang. "A backstepping global fast terminal sliding mode control for trajectory tracking control of industrial robotic manipulators." IEEE Access 9 (2021): 31921-31931.

[10] Vo, Anh Tuan, and Hee-Jun Kang. "A chattering-free, adaptive, robust tracking control scheme for nonlinear systems with uncertain dynamics." IEEE Access 7 (2019): 10457-10466.

[11] Y. Fan, K. Xing, and X. Jiang, “Fuzzy adaptation algorithms’ control for robot manipulators with uncertainty modelling errors,” Complexity, vol. 2018, pp. 1–8, 2018.

[12] J. Na, Y. Huang, X. Wu, S.-F. Su, and G. Li, “Adaptive finite time fuzzy control of nonlinear active suspension systems with input delay,” IEEE Transactions on Cybernetics, vol. 50, no. 6, pp. 2639–2650, 2019.

[13] S. Wang and J. Na, “Parameter estimation and adaptive control for servo mechanisms with friction compensation,” IEEE Transactions on Industrial Informatics, p. 1, 2019.

[14] Ghaleb, Nasr M., and Ayman A. Aly. "Modeling and control of 2-DOF robot arm." International Journal of Emerging Engineering Research and Technology 6, no. 11 (2018): 24-31.
[15] Ashagrie, Aderajew, Ayodeji OlalekanSalau, and Tilahun Weldcherkos. "Modeling and control of a 3-DOF articulated robotic manipulator using self-tuning fuzzy sliding mode controller." Cogent Engineering 8, no. 1 (2021): 1950105.
[16] Zeghlache, Samir, Hemza Mekki, Abderrahmen Bouguerra, and Ali Djerioui. "Actuator fault tolerant control using adaptive RBFNN fuzzy sliding mode controller for coaxial octorotor UAV." ISA transactions 80 (2018): 267-278.
[16] Zheng, Zewei, and Liang Sun. "Adaptive sliding mode trajectory tracking control of robotic airships with parametric uncertainty and wind disturbance." Journal of the Franklin Institute 355, no. 1 (2018): 106-122.
[17] Li, Ang, Ming Liu, and Yan Shi. "Adaptive sliding mode attitude tracking control for flexible spacecraft systems based on the Takagi-Sugeno fuzzy modelling method." Acta Astronautica 175 (2020): 570-581.
[17] Sakthivel, Rathinasamy, S. Harshavarthini, Ramasamy Kavikumar, and Yong-Ki Ma. "Robust tracking control for fuzzy Markovian jump systems with time-varying delay and disturbances." IEEE Access 6 (2018): 66861-66869.
[18] Zhu, Yunkai, and JuntaoFei. "Disturbance observer based fuzzy sliding mode control of PV grid connected inverter." IEEE Access 6 (2018): 21202-21211.
[19] Xie Y, Tang X, Song B, Zhou X, Guo Y. Model-free tuning strategy of fractional-order PI controller for speed regulation of permanent magnet synchronous motor. Trans Inst Meas Control 2019;41(1):23–35.
[20] Yousuf, Bilal M., Abdul Saboor Khan, and Aqib Noor. "Multi-agent tracking of non-holonomic mobile robots via non-singular terminal sliding mode control." Robotica 38, no. 11 (2020): 1984-2000.
[21] Das, Madhu Sudan, Anu Samanta, Sourish Sanyal, and Sanjoy Mandal. "AKH-NFIS: Adaptive Krill Herd Network Fuzzy Inference System for Mobile Robot Navigation." Wireless Personal Communications (2021): 1-
[22] Yousuf, Bilal M., Abdul Saboor Khan, and Aqib Noor. "Multi-agent tracking of non-holonomic mobile robots via non-singular terminal sliding mode control." Robotica 38, no. 11 (2020): 1984-2000.

Conflict of Interest

The author declares no potential conflict of interest with respect to the authorship and/or publication of this article.

Funding

No funding was received

Data Availability Statement

No associated data.